Received: November 5, 2013 | Accepted: December 10, 2013 | Web Released: December 14, 2013 CL-131037

Delayed Fluorescence Behaviors of Aminopyridine Oligomers: Azacalix[*n*](2,6)pyridines ($n = 3$ and 4) and Their Linear Analog

Natsuko Uchida,[1,4] Tohru Sato,[2,3] Junpei Kuwabara,[1,4] Yoshinobu Nishimura,[1,5] and Takaki Kanbara*[1,4]

[1]*Tsukuba Research Center for Interdisciplinary Materials Science (TIMS), Graduate School of Pure and Applied Sciences, University of Tsukuba, 1-1-1 Tennodai, Tsukuba, Ibaraki 305-8573*

[2]*Department of Molecular Engineering, Graduate School of Engineering, Kyoto University, Katsura, Kyoto 615-8510*

[3]*Elements Strategy Initiative for Catalysts and Batteries (ESICB), Kyoto University, Katsura, Kyoto 615-8510*

[4]*Institute of Materials Science, Graduate School of Pure and Applied Sciences, University of Tsukuba, 1-1-1 Tennodai, Tsukuba, Ibaraki 305-8573*

[5]*Department of Chemistry, Graduate School of Pure and Applied Sciences, University of Tsukuba, 1-1-1 Tennodai, Tsukuba, Ibaraki 305-8573*

(E-mail: kanbara@ims.tsukuba.ac.jp)

Aminopyridine oligomers exhibited long-lived emission at 77 K, which could be assigned to the delayed fluorescence. The macrocyclic structure predominantly dictated the emission behaviors. Their emission behaviors were elucidated from time-dependent density functional theory calculations.

The luminescence mechanism of organic compounds can be classified into fluorescence, phosphorescence, and delayed fluorescence. Delayed fluorescence is an emission process that proceeds via up-conversion from the first excited triplet state (T_1) to the first excited singlet state (S_1) through reverse intersystem crossing (RISC).[1,2] It can be classified into two types of mechanisms because of up-conversion through RISC: (i) triplet–triplet annihilations and (ii) thermally activated delayed fluorescence (TADF, also called E-type delayed fluorescence).

In 2009, the Adachi group realized the first application of TADF materials for proposing the third-generation OLEDs (organic light-emitting diodes), which are expected to show an excellent electroluminescence efficiency with good stability in high current density.[1] Although the phenomena of delayed fluorescence has been known from 1950s,[3] TADF materials draw renewed attention since their report.[4] In the TADF mechanism, a key factor is how to achieve a small energy gap between the singlet and triplet states (ΔE_{ST}) to enable an up-conversion of the triplet exciton from a triplet to a singlet state. It has been proposed that the molecular design for achieving a small ΔE_{ST} includes a donor–acceptor framework to induce an intramolecular charge-transfer transition from separate HOMO to LUMO levels in a single molecule.[5] However, this molecular design for TADF compounds should involve an appropriate selection of donor and acceptor units. The development of another design for the delayed fluorescence compounds, in addition to the conventional design, will expand the scope of TADF materials.

Herein, we report the first observation of delayed fluorescence behavior of macrocyclic and acyclic aminopyridine oligomers **1**–**3**, which depends on the size and topology of the recurring units (Figure 1). Azacalix[*n*](2,6)pyridines are macrocyclic aminopyridine[6] oligomers.[7,8] Although the structural features and reactivity of the azacalix[*n*](2,6)pyridines have been investigated,[7–9] the fundamental luminescence properties of the compounds have not been well evaluated. Time-dependent density functional theory (TD-DFT) calculations were also performed to elucidate their luminescence behaviors. The insight would provide novel and valuable information for the molecular design of delayed fluorescence compounds.

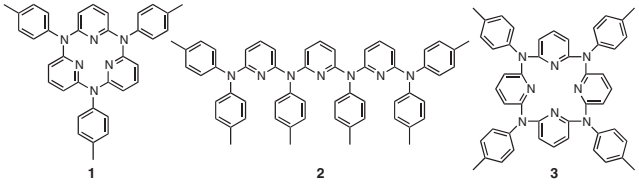

Figure 1. Molecular structures of **1**–**3**.

Azacalix[*n*](2,6)pyridine derivatives **1** ($n = 3$) and **3** ($n = 4$) were synthesized by a method described in the literature.[9] Linear chain compound **2** was obtained in high yields by multistep synthesis (Scheme S1).[10] The UV–vis absorption spectra and emission spectra of **1**–**3** in 2-methyltetrahydrofuran (Me-THF) solutions at both room temperature and 77 K are shown in Figure 2. The emission quantum yields (Φ_{em}) of **1**, **2**, and **3** at room temperature were 27%, 45%, and 8%, respectively, whereas the corresponding Φ_{em} values of **1**–**3** were increased to 38%, 56%, and 67% at 77 K. The details of the emission lifetimes (τ) of **1**–**3** are summarized in Table S1, and the emission-decay curves are shown in Figure 3. At room temperature, **1**–**3** showed a blue emission with a maximum emission wavelength (λ_{em}) of around 420 nm. In a glass matrix at 77 K, the emissions of **1**–**3** appeared at virtually the same wavelength of 420 nm as those at room temperature, whereas **2** and **3** showed new emissions of around 570 nm at 77 K. These 570-nm emissions of **2** and **3** consist of one component, which was confirmed from their emission-decay curves. The emission-decay curves of **1**–**3** around 420 nm suggest that the emission consists of two components with different lifetimes at both room temperature and 77 K.[11] It should be noted that in a glass matrix at 77 K, the lifetimes for the emission of **1**–**3** were quite long; τ was in the several hundred ms range (Table S1 and Figure S1). To clarify the spectra of the long-lived emission components, the time-dependent PL measurements for the long-lifetime component were carried out at 77 K (Figure S3). The delayed emissions of **1**–**3** at 420 nm appeared to have almost the same spectra as the normal PL spectra at 77 K.

Because delayed fluorescence proceeds through an up-conversion from a triplet state to a singlet state, the emission

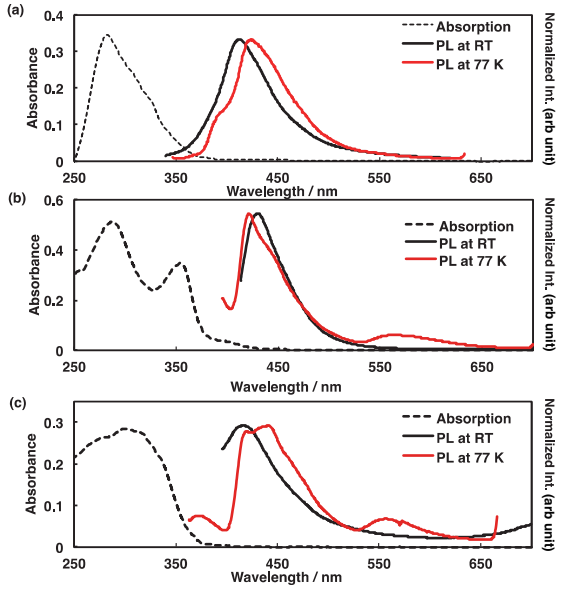

Figure 2. UV–vis absorption spectra and photoluminescence spectra of (a) **1** (at RT and 77 K both $\lambda_{ex} = 320$ nm), (b) **2** (at RT and 77 K both $\lambda_{ex} = 360$ nm) and (c) **3** (at RT: $\lambda_{ex} = 370$ nm, at 77 K: $\lambda_{ex} = 340$ nm) in degassed Me-THF solution of 1.0×10^{-5} M.

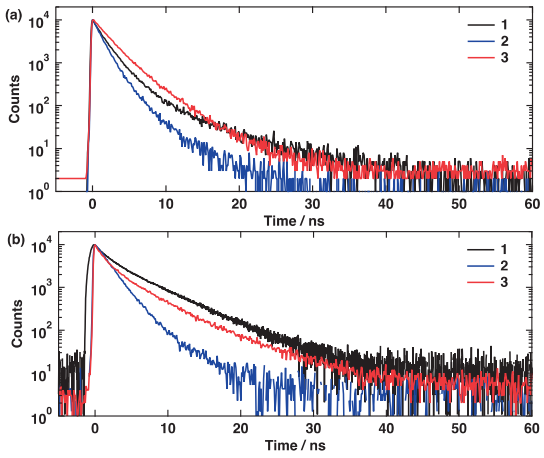

Figure 3. Emission-decay curves of **1**–**3** in degassed Me-THF solution of 1.0×10^{-5} M (a) at RT of **1** ($\lambda_{ex} = 380$ nm, $\lambda_{em} = 422$ nm, black line), **2** ($\lambda_{ex} = 380$ nm, $\lambda_{em} = 441$ nm, blue line), **3** ($\lambda_{ex} = 360$ nm, $\lambda_{em} = 421$ nm, red line) (b) at 77 K glass matrix state of **1** ($\lambda_{ex} = 373$ nm, $\lambda_{em} = 422$ nm, black line), **2** ($\lambda_{ex} = 373$ nm, $\lambda_{em} = 441$ nm, blue line) and **3** ($\lambda_{ex} = 360$ nm, $\lambda_{em} = 421$ nm, red line).

spectrum of the delayed fluorescence is generally similar to the corresponding fluorescence spectrum.[2] For the **1**–**3** compounds, the long-lived emission spectra around 420 nm were almost same as those of fluorescence spectra. In addition, it was confirmed that the blue emission around 420 nm includes two emission components with different emission lifetime ranges at 77 K. The long-lived emission at 420 nm at low temperatures (Table S1, τ_3 of 77 K) of **1**–**3** can therefore be categorized into

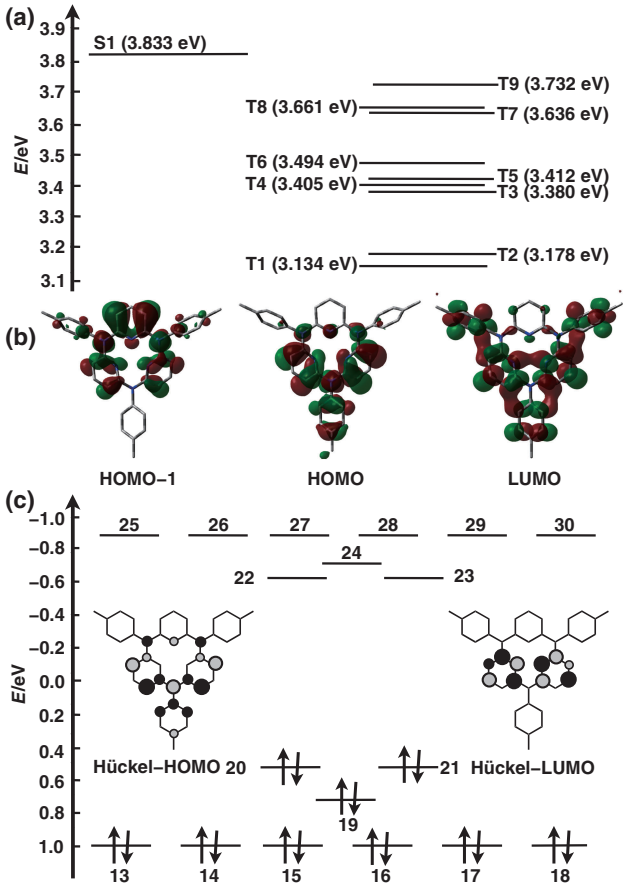

Figure 4. (a) Energy diagram of **1**. (b) Pictorial representations of the frontier MOs of **1**. Calculated at the PBE0/6-31G(d,p) level of theory. (c) Energy diagram of **1** within Hückel approximation (The Coulomb integrals of nitrogen of amino group and pyridine moiety and the resonance integrals were taken from reference[14]).

delayed fluorescence and fast emissions (Table S1, τ_1 and τ_2 of 77 K) at the same wavelength as that of fluorescence.

For a large difference among **1**, **2**, and **3** at 77 K, **2** and **3** exhibit a new long-lived emission peak around 570 nm in addition to the emission at 420 nm (Table S1 and Figure S3). The results of time-dependent PL behaviors suggest that the emissions at 570 nm indicate phosphorescence; the phosphorescence of an organic compound generally appears in a longer wavelength region than the fluorescence spectrum at 77 K.[2] The Φ_{em} value also suggests the involvement of phosphorescence, because the Φ_{em} values of **2** and **3** increase with a decrease in temperature. Similar PL behavior was previously reported for proflavine hydrochloride, which is a delayed fluorescence compound.[12] From the maximum emission wavelength of phosphorescence and fluorescence, ΔE_{ST} of **2** and **3** were observed to be 0.77 and 0.60 eV, respectively. In **1**, it can be assumed that ΔE_{ST} is nearly 0 eV because no phosphorescence was observed. Even for the same recurring aminopyridine unit, different conformations and numbers of ring sizes lead to different ΔE_{ST} values and phosphorescence behaviors.

Next, TD-DFT calculations for **1**–**3** were carried out using Gaussian 09.[13] The PBE0 functional with the 6-31G(d,p) basis

set was employed; the PBE0 functional well reproduced the experimental absorption wavelength of **1** (Figure S4 and Table S2). The calculated ΔE_{ST} at the Franck–Condon states of **2** and **3** were 0.72 and 0.65 eV, respectively, which are in good agreement with the experimental ΔE_{ST} values of **2** and **3** (0.77 and 0.60 eV), as estimated from the fluorescence and phosphorescence wavelengths discussed above. For **1**, on the other hand, the calculated ΔE_{ST} is 0.70 eV, while the experimental ΔE_{ST} was almost 0 eV, because no phosphorescence was observed.

From the TD-DFT calculations, we propose a plausible mechanism of the observed delayed fluorescence in **1**–**3**. Figure 4a shows the energy diagram of **1**, whereas Figures S5a and S5b show the energy diagrams of **2** and **3**, respectively. It should be noted that **1**–**3** have quasi-degenerate excited triplet states T_n (where $n = 7$, 8, and 9 for **1**; $n = 9$, 10, 11, and 12 for **2**; and $n = 9$ and 10 for **3**) near the lowest excited singlet state S_1. The energy gap between S_1 and the quasi-degenerate T_n states of **1**–**3** close to S_1 is less than 240 meV; thus, the energy barriers can be overcome by thermal excitation via RISC. In contrast, the energy gaps between S_1 and T_1 of **1**, **2**, and **3** are too large to be overcome through thermal excitation. Therefore, delayed fluorescence via the T_1 states seems to be almost impossible. These results suggest that the observed delayed fluorescence originates from the higher quasi-degenerate triplet states T_n. According to the energy diagram of **1** within the Hückel approximation, these quasi-degenerate states of **1**–**3** are due to the nonbonding orbitals formed by the *meta*-linkage of the pyridine ring through the amino groups (Figure 4c);[15] these T_n states close to the S_1 states are excitations between the orbitals localized on the tolyl and pyridine moieties (see the MOs of Figures 4b and 4c). The T_1 state of **1** is an excitation from the HOMO mainly localized on the remaining pyridine moieties to the LUMO. Therefore, the overlap density between T_1 and T_9 is small because the region where the HOMO is localized differs from the region where the next HOMO (HOMO−1) is localized (Figure 4b). The difference in the phosphorescence behavior of **1**–**3** indicates that the orbital localization of the quasi-degenerate excited triplet states might be somewhat weak in **2** and **3**.[16]

In conclusion, we observed the delayed fluorescence behavior in **1**–**3**. The TD-DFT calculations indicate that each of them has a small energy gap, ΔE_{ST}, between the fluorescence state S_1 and the higher excited quasi-degenerate triplet state T_n than the T_1 state. The macrocyclic structure of **1** predominantly dictated the photoluminescence properties. To clarify this peculiarity in **1**, further theoretical calculations for the excited states are required. We will discuss the results in another report in the near future.

The authors kindly acknowledge the emission lifetime measurements provided by HORIBA, Ltd. We appreciate the help received from S. Mimura, Dr. Y. Nakata, and S. Akaji of HORIBA, Ltd., with the emission lifetime measurements. Prof. Dr. T. Nabeshima and Dr. M. Yamamura are grateful for the support provided during quantum yield measurements and long-term photoluminescence spectra measurements. Numerical calculations were performed partly at the Supercomputer Laboratory of Kyoto University and the Research Center for Computational Science, Okazaki, Japan.

References and Notes

1 A. Endo, M. Ogasawara, A. Takahashi, D. Yokoyama, Y. Kato, C. Adachi, *Adv. Mater.* **2009**, *21*, 4802.
2 B. Valeur, M. N. Berberan-Santos, *Molecular Fluorescence: Principles and Applications*, 2nd ed., Wiley-VCH, **2012**. doi:10.1002/9783527650002.
3 a) R. Williams, *J. Chem. Phys.* **1958**, *28*, 577. b) H. Sponer, Y. Kanda, L. A. Blackwell, *J. Chem. Phys.* **1958**, *29*, 721. c) C. A. Parker, C. G. Hatchard, *Trans. Faraday Soc.* **1961**, *57*, 1894. d) C. A. Parker, *Nature* **1963**, *200*, 331. e) C. A. Parker, C. G. Hatchard, *Trans. Faraday Soc.* **1963**, *59*, 284. f) C. A. Parker, *Spectrochim. Acta* **1963**, *19*, 989. g) R. G. Kepler, J. C. Caris, P. Avakian, E. Abramson, *Phys. Rev. Lett.* **1963**, *10*, 400.
4 a) A. Endo, K. Sato, K. Yoshimura, T. Kai, A. Kawada, H. Miyazaki, C. Adachi, *Appl. Phys. Lett.* **2011**, *98*, 083302. b) S. Y. Lee, T. Yasuda, H. Nomura, C. Adachi, *Appl. Phys. Lett.* **2012**, *101*, 093306. c) H. Tanaka, K. Shizu, H. Miyazaki, C. Adachi, *Chem. Commun.* **2012**, *48*, 11392. d) Q. Zhang, J. Li, K. Shizu, S. Huang, S. Hirata, H. Miyazaki, C. Adachi, *J. Am. Chem. Soc.* **2012**, *134*, 14706. e) F. A. Salazar, A. Fedorov, M. N. Berberan-Santos, *Chem. Phys. Lett.* **1997**, *271*, 361. f) M. N. Berberan-Santos, J. M. M. Garcia, *J. Am. Chem. Soc.* **1996**, *118*, 9391. g) S. Park, O.-H. Kwon, Y.-S. Lee, D.-J. Jang, S. Y. Park, *J. Phys. Chem. A* **2007**, *111*, 9649. h) R. Czerwieniec, J. Yu, H. Yersin, *Inorg. Chem.* **2011**, *50*, 8293.
5 H. Uoyama, K. Goushi, K. Shizu, H. Nomura, C. Adachi, *Nature* **2012**, *492*, 234.
6 a) T. W. Bell, A. B. Khasanov, M. G. B. Drew, *J. Am. Chem. Soc.* **2002**, *124*, 14092. b) J.-D. Cheon, T. Mutai, K. Araki, *Org. Biomol. Chem.* **2007**, *5*, 2762.
7 a) Y. Miyazaki, T. Kanbara, T. Yamamoto, *Tetrahedron Lett.* **2002**, *43*, 7945. b) T. Kanbara, Y. Suzuki, T. Yamamoto, *Eur. J. Org. Chem.* **2006**, 3314. c) N. Uchida, A. Taketoshi, J. Kuwabara, T. Yamamoto, Y. Inoue, Y. Watanabe, T. Kanbara, *Org. Lett.* **2010**, *12*, 5242. d) N. Uchida, J. Kuwabara, A. Taketoshi, T. Kanbara, *J. Org. Chem.* **2012**, *77*, 10631.
8 a) E.-X. Zhang, D.-X. Wang, Q.-Y. Zheng, M.-X. Wang, *Org. Lett.* **2008**, *10*, 2565. b) H.-Y. Gong, Q.-Y. Zheng, X.-H. Zhang, D.-X. Wang, M.-X. Wang, *Org. Lett.* **2006**, *8*, 4895.
9 Y. Suzuki, T. Yanagi, T. Kanbara, T. Yamamoto, *Synlett* **2005**, 263.
10 Supporting Information is available electronically on the CSJ-Journal Web site, http://www.csj.jp/journals/chem-lett/index.html.
11 Similar case was reported: C.-S. Choi, K.-S. Jeon, K.-H. Lee, *J. Photosci.* **2004**, *11*, 71.
12 C. A. Parker, C. G. Hatchard, *J. Phys. Chem.* **1962**, *66*, 2506.
13 M. J. Frisch, et al., *Gaussian 09 (Revision D.01)*, see Supporting Information.
14 A. Streitwieser, *Molecular Orbital Theory for Organic Chemists*, John Wiley & Sons, **1961**.
15 E. Heilbronner, H. Bock, *The HMO Model and Its Application: Basis and Manipulation*, John Wiley & Sons, **1976**, Vol. 1.
16 T. Sato, M. Uejima, N. Iwahara, N. Haruta, K. Shizu, K. Tanaka, *J. Phys.: Conf. Ser.* **2013**, *428*, 012010.

